

The Impact of Different Levels of In-Place Density on Asphalt Pavement Performance

DOT Office

State Materials Office

Research Report Number

FL/DOT/SMO/18-589

Authors

Wayne Allick, Jr.
Bouzid Choubane
Ohhoon Kwon
David Hernando

Publication Date

August 2018

TABLE OF CONTENTS

EXECUTIVE SUMMARY	4
1 INTRODUCTION	5
2 OBJECTIVE	6
3 FLORIDA'S APT PROGRAM	7
3.1 Experimental Design	7
4 DATA COLLECTION	9
4.1 Rut Depth Measurements	9
4.2 In-Place Density Measurements	10
4.3 Indirect Tensile Strength Measurements	10
4.4 Cantabro Abrasion Loss Measurements	10
4.5 Surface Macrotexture Measurements	11
4.6 Surface Friction Measurements	13
5 RESULTS AND DISCUSSION	14
5.1 Impact of In-Place Density on Rutting	14
5.2 Impact of In-Place Density on Cracking Resistance	15
5.3 Impact of In-Place Density on Raveling Resistance	16
5.4 Impact of In-Place Density on Pavement Surface Macrotexture and Friction	18
6 SUMMARY AND CONCLUSIONS	22
ACKNOWLEDGEMENTS	23
REFERENCES	24
APPENDIX	26

LIST OF FIGURES

Figure 1. Cross-Sections of the Test Sections	8
Figure 2. Path of Laser Profiler for Measuring Pavement Surface Profiles	9
Figure 3. Test Section Layout and Core Density Results	10
Figure 4. Comparison of 6-inch vs. 4-inch Diameter Specimens after Cantabro Loss Testing ...	11
Figure 5. HVS Loading Area with Texture Measurement Segments	12
Figure 6. Schematic of Texture Measurements	12
Figure 7. Obtaining Friction Measurements with the DFT.....	13
Figure 8. Progression of Rutting Performance in the Test Sections	14
Figure 9. Transverse Rut Profiles at 100,000 HVS Wheel Passes.....	15
Figure 10. In-Place Density vs Indirect Tensile Strength	16
Figure 11. In-Place Density vs. Cantabro Loss After HVS Testing.....	17
Figure 12. Pavement Surface Macrottexture and Friction Before and After HVS Testing	18
Figure 13. Correlation between In-Place Density and MPD	19
Figure 14. Distribution of MPD on the Test Sections Before HVS Testing.....	20
Figure 15. Core Specimens after Cantabro Testing.....	26

LIST OF TABLES

TABLE 1. Rut Depth Deformation and Densification Summary.....	15
TABLE 2. Cantabro Abrasion Loss Results.....	17
TABLE 3. Descriptive Statistics for MPD Data.....	19
TABLE 4. Robust Test of Equality of Mean MPD	20
TABLE 5. Pair-Wise Multiple Comparison of MPD Before HVS Testing	21
TABLE 6. Pair-Wise Multiple Comparison of MPD After HVS Testing.....	21
TABLE 7. Indirect Tensile Strength Results	26
TABLE 8. Friction Data from DFT Testing.....	27
TABLE 9. Aggregate Gradation of Plant Mix Sampled at Test Section 1	28
TABLE 10. Aggregate Gradation of Plant Mix Sampled at Test Section 2	29
TABLE 11. Aggregate Gradation of Plant Mix Sampled at Test Section 3	30
TABLE 12. Asphalt Binder Laboratory Test Results.....	31

EXECUTIVE SUMMARY

In-place air void content or density is an important factor that affects the performance of the pavement throughout its service life. Therefore, it is of importance to ensure that the in-place density of a pavement is within an acceptable range. However, it is not always clear how much density should be practically specified and achieved during construction to assure optimum pavement performance. Consequently, the Florida Department of Transportation (FDOT) conducted a full-scale study at its Accelerated Pavement Testing (APT) facility to assess the impact of different in-place density levels on asphalt pavement performance. Three test sections having similar underlying condition and asphalt mixture were constructed. A typical 12.5-mm fine-graded asphalt mixture used in Florida with a PG 76-22 binder mixture was placed at target in-place densities of 87%, 90%, and 93%, respectively while complying with all the other standard FDOT construction and materials specifications and methods.

The findings of this study showed that higher in-place density improved asphalt pavement rutting performance, and produces higher indirect tensile strength (IDT) which is indicative of better cracking resistance. The Mean Profile Depth (MPD) data collected showed that the pavement surface macrotexture reduces with higher in-place density. In addition, the test section with the highest in-place density had, comparatively, the lowest MPD value before and after HVS testing. Results from the Dynamic Friction Tester revealed that higher in-place density did not provide any improvement in friction characteristics. Cantabro loss results indicated that higher in-place density resulted in the lowest material loss which is indicative of better raveling resistance.

1 INTRODUCTION

In-place air void content or density is an important factor that affects the long-term performance of asphalt pavements. High air void content in a finished pavement will adversely affect its durability and performance in various ways. High in-place air voids can allow air filtration into an asphalt layers and, thus, accelerates the aging or hardening process of the asphalt binder through oxidation. It can, in addition, allow the penetration of excessive amounts of water inducing stripping of the asphalt binder from the aggregates. High in-place air void content can also result in excessive densification under traffic. Therefore, it is of importance to ensure that the air voids of an as-constructed asphalt layer are within an acceptable range (1). As such, many transportation agencies specify minimum pavement density requirements during construction. It is not, however, always clear how much density should be practically specified and achieved during construction to assure optimum pavement performance.

In 1989, Brown and Cross reported poor correlation between in-place rutting and low air voids, and that indirect tensile strength values were not significantly related to rutting based on data from five field projects (2). However, of the five projects considered in their investigation, three were constructed in 1982, one in 1980, and the other in 1972. These pavements experienced years of traffic loading prior to sampling pavement cores for the study. It is possible that the resulting laboratory test findings may not have reflected the as-constructed properties of the asphalt mixtures.

In 2002, researchers investigated the effect of as-constructed air void content on asphalt pavement performance using the LTPP database. It was found, though, that the LTPP database did not contain sufficiently suitable as-constructed data satisfying the selection criteria (3). Because of this limitation, no reasonable models or compaction guidelines were developed to relate as-constructed air voids to pavement performance.

In 2013, Zeinali et al. evaluated the effect of density on rutting and fatigue performance on five asphalt pavement projects in Kentucky (4). The in-place densities were determined using non-nuclear gauges. The measurements indicated that the average in-place density on the projects were 88.5, 89.3, 86.8, 88.4, and 89.3%, respectively. All the mixtures were 9.5-mm nominal maximum

aggregate size (NMAS). In addition, a performance grade (PG) 76-22 binder was used on three of the projects while PG 64-22 binder was used on the other two projects. They reported that 33 to 115% increase in rutting resistance could have been achieved by compacting pavements to 92% density. The researchers did not find a statistically significant difference in fatigue life with increasing density using the flexural beam fatigue test results (4). One should note, that the small range of in-place densities evaluated may be within the margin of error of the non-nuclear gauge utilized in the study (5).

In 2015, Wang et al. investigated the effect of variations in in-place density on 55 project sites using performance data collected by the New Jersey Department of Transportation (NJDOT) (6). They used the Surface Distress Index (SDI) to evaluate pavement deterioration on the projects. However, a statistically significant explanation was not found between the variation in pavement service life and air void contents in the asphalt surface and intermediate layers, respectively. They developed a performance-related pay adjustment for NJDOT using results from a life-cycle cost analysis (LCCA). Their LCCA combined the effect of air voids from the surface and intermediate layers to estimate the impact of in-place air voids on expected pavement service life. The LCCA in this study did not consider asphalt layer thickness.

The studies noted above faced challenges with varying subsurface conditions, asphalt layer thicknesses, environmental conditions, and traffic loading which are critical when comparing the impact of in-place density on asphalt pavement performance.

2 OBJECTIVE

The primary objective of this study was to determine the impact of in-place density on asphalt pavement performance. To allow for a faster and a more practical assessment under closely simulated and controlled in-service conditions, a full-scale accelerated pavement testing (APT) was considered. Three asphalt test sections having similar underlying condition were constructed with a typical Florida fine-graded mix design. The mixtures were 12.5-mm NMAS, with a PG 76-22 binder. The test sections were compacted to three target in-place densities of 87%, 90%, and 93%, respectively, while complying with all the other standard FDOT construction and materials specifications and methods.

3 FLORIDA'S APT PROGRAM

FDOT initiated an APT program in early 2000. The APT and research program is based within the State Materials Research Park in Gainesville, Florida. The testing site consists of five linear test tracks each measuring approximately 450-foot-long by 12-foot-wide, and three additional tracks measuring approximately 150-foot-long by 12-foot-wide. There are additional two test tracks designed with water-table control capabilities within the supporting base layers. The accelerated loading is performed using a Heavy Vehicle Simulator (HVS). All tests are conducted at a controlled temperature of 50°C at a depth of 2-inches from the pavement surface. Rut depth measurements are taken periodically using a laser profiling system mounted on both sides of the underside of the HVS wheel carriage. The working of this system as well as a complete description of the test facility have been described elsewhere (7, 8).

3.1 Experimental Design

In this experiment, the asphalt layer of an existing 450-foot-long and 12-foot-wide test lane was milled and resurfaced. A 1-inch thick asphalt layer remained after milling. The lane was resurfaced with two 1.5-inch thick layers of a 12.5-mm NMAAS asphalt mixture with a PG 76-22 binder. The supporting layers consisted of a 10.5-inch limerock base over a 12-inch limerock stabilized subgrade.

The asphalt mixture layers were placed using a double drum steel wheeled roller in both vibratory and static modes. The first 1.5-inch thick layer was compacted to 93% density throughout the test lane. Thereafter, the lane was divided into three test sections. Subsequently, the second 1.5-inch thick surface mixture along the three test sections was compacted to target in-place densities of 87%, 90%, and 93%, respectively. The in-place density of the compacted pavement was controlled with a non-nuclear density gauge and measured by recovering cores from the pavement after construction.

Each of the test section was further divided into three replicate test segments for a total of nine distinct test segments or areas. The intent of these three replicate areas within each test section as well the randomness in the testing sequence within the test lane was to allow for a statistically sound experiment design. Figure 1 illustrates the structural components of each of these test

sections. As previously noted, the test sections were constructed in accordance with all the standard FDOT construction and materials specifications and methods.

As with previous experiments, all testing was performed at a controlled temperature of 50°C at a depth of 2-inches from the pavement surface. All test sections were loaded until a rut depth of 0.5 inches was accumulated or the resulting rutting had stabilized and the rate of rutting appeared to be constant, whichever came first. The load was applied uni-directionally through a Goodyear G165 (12-inch wide) super-single tire loaded to 9,000 lbs. at a speed of 8 mph, with a 4-inch lateral wheel wander. The reasoning for such a loading configuration was provided elsewhere (8). Automated three-dimensional (3-D) surveys of the resulting ruts were conducted at predetermined loading intervals on each of the test areas.

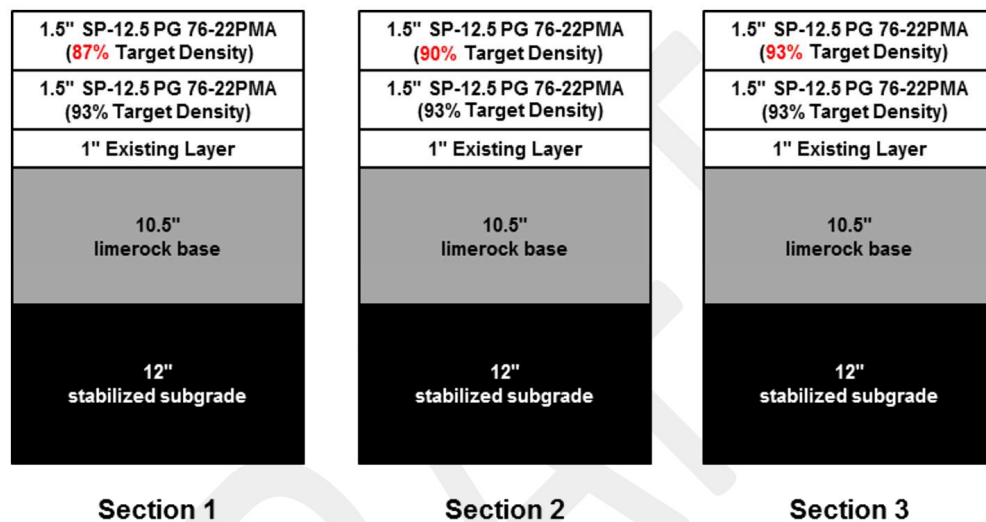


Figure 1. Cross-Sections of the Test Sections

4 DATA COLLECTION

4.1 Rut Depth Measurements

Rut measurements were collected at predetermined intervals in the form of longitudinal and transverse profiles during this study. These longitudinal and transverse profiles were then numerically integrated to form a 3-D surface plot of the test section. The profiles were automatically acquired using a laser-based system installed on the HVS loading assembly/carriage as previously described.

At each predetermined number of load passes, the profile measurements were taken following a directional pattern as shown in Figure 2. In such a pattern, the lasers, while traveling with the “unloaded” carriage, surveyed an area of approximately 20-ft in length and 5-ft in width in a series of 61 fluid and continuous sweeps. The data was collected at a rate of 16000 Hz and averaged at 4-inch intervals. Following this process, a total of 58 transverse profiles are generated, at any given number of load passes. The initial profile (profile after construction and before HVS testing) was used as the reference (baseline) to estimate the rut depths for this study.

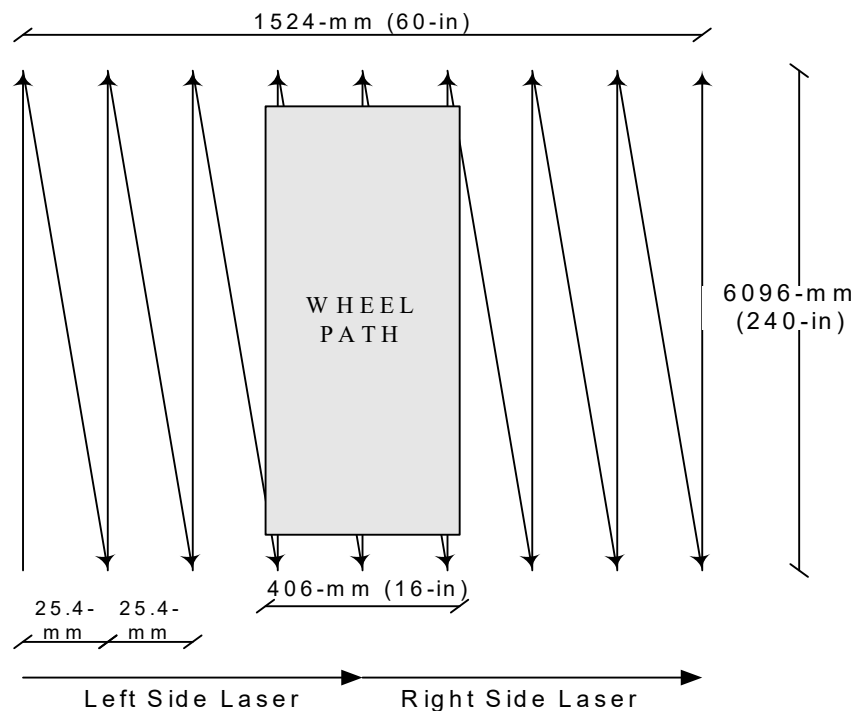


Figure 2. Path of Laser Profiler for Measuring Pavement Surface Profiles

4.2 In-Place Density Measurements

The density of the surface course within each test section shortly after construction was measured using asphalt core samples tested in accordance with FM1–T166 (9). The test results indicated that the average in-place densities were within $\pm 1\%$ from the respective target values of 87%, 90%, and 93%. Figure 3 shows the layout of the core locations on the test lane as well as their corresponding values.

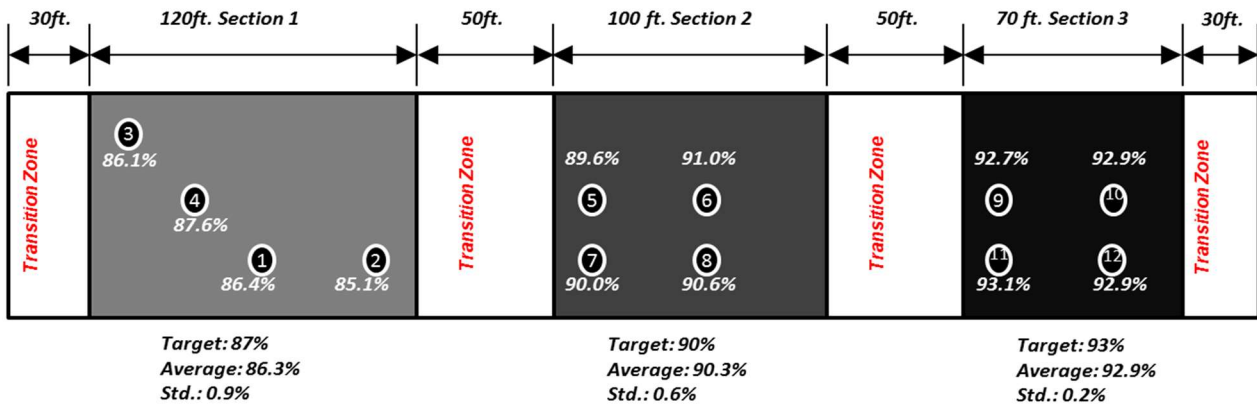


Figure 3. Test Section Layout and Core Density Results

4.3 Indirect Tensile Strength Measurements

Cracking performance of asphalt pavements is of interest to Florida since top-down cracking is the primary distress on its State roadways. Khosla and Harvey reported that the life of asphalt mixtures decreases exponentially with decreasing tensile strength, and that rut depths decrease with increasing tensile strength (10). Therefore, IDT strength testing was conducted in accordance with ASTM D6931 on core samples randomly obtained within each test section shortly after construction. The test results were used to evaluate the impact of in-place pavement density on cracking resistance.

4.4 Cantabro Abrasion Loss Measurements

The Cantabro Abrasion Loss test is typically conducted to evaluate the durability of open-graded friction course (OGFC) mix designs using the L.A. abrasion machine in accordance with AASTHO TP-108. The test results are interpreted as an indirect measure of raveling potential of OGFC mixtures (11). However, Doyle and Howard investigated the durability of dense graded mixtures with recycled-asphalt pavement (RAP) using the Cantabro loss method on 6-inch diameter

laboratory compacted specimens. They concluded that the test shows promise for dense graded mixtures as well (12).

Preliminary testing was conducted on 6-inch diameter cores which were trimmed to isolate the 1.5-inch thick surface layer in each test section. Those specimens typically broke into half pieces before reaching 60 revolutions in the L.A. abrasion machine without the use of a charge. The damage observed on the specimens may be attributed to the aspect-ratio. Consequently, three 4-inch diameter core specimens were obtained from each test section before and after HVS testing to perform Cantabro loss testing.



Figure 4. Comparison of 6-inch vs. 4-inch Diameter Specimens after Cantabro Loss Testing

After each specimen was individually rotated in the Los Angeles machine at about 30 revolutions per minute for 300 revolutions its weight was recorded to measure the loss of mass after testing. The results were used to evaluate the relative impact of in-place density on the raveling resistance of the asphalt mixture.

4.5 Surface Macrotexture Measurements

Previous studies have shown that asphalt pavement surface macrotexture has a significant influence on noise levels generated from tire/pavement interaction (13). The mean profile depth (MPD) is a standard measure of the pavement surface macrotexture. Rezaei and Harvey reported that higher MPD on dense graded pavement corresponded to higher noise level at low frequencies (14). The MPD data in this study were obtained in each test section using a Circular Texture Meter (CTM) in accordance with ASTM E2157.



Figure 5. HVS Loading Area with Texture Measurement Segments

The HVS loading areas were divided into fifteen 17×17 -inch areas as shown in Figure 5. The average MPD value within each area includes four overlapping CTM measurements as shown in Figure 6. The MPD was collected in this study to determine whether in-place density significantly impacts asphalt pavement surface macrotexture, which may contribute to the noise generated by tire-pavement interaction.

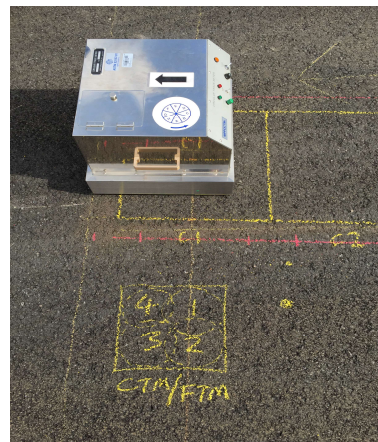
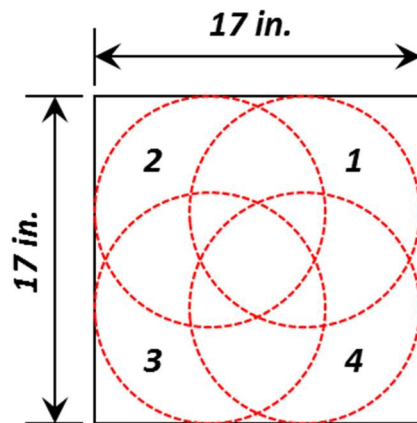


Figure 6. Schematic of Texture Measurements

4.6 Surface Friction Measurements

The pavement surface frictional properties in each test section were measured using a Dynamic Friction Tester (DFT) and converted to the friction number obtained at the standard test speed of 40 mph using the locked-wheel tester with a ribbed tire (FN40R). In a previous FDOT study, correlations were developed between the friction measurements obtained at different vehicle speed and DFT data (15). A coefficient of determination (R^2) of 0.85 was determined for the linear regression between the locked-wheel tester with a ribbed tire at a speed of 40 mph (FN40R) and the DFT coefficient at 65 km/h (40 mph) on dense-graded asphalt mixtures. The DFT friction coefficient collected at 65 km/h (40 mph) is designated as DFT40. Equation 1 shown below was developed in that study to convert DFT friction coefficient results to FN40R.

$$FN40R = 0.88 * DFT40 + 4.74 \quad \text{Equation 1}$$

Three DFT measurements were obtained before HVS testing then after 10,000 and 100,000 HVS wheel passes for a total of nine measurements in each test section. Figure 7 shows the collection of DFT data on a test section.

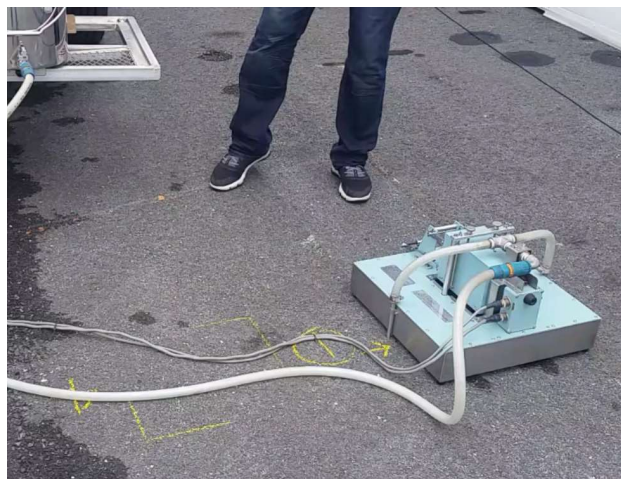


Figure 7. Obtaining Friction Measurements with the DFT

5 RESULTS AND DISCUSSION

The HVS laser profile system was used to capture the progression of rutting in each loading area during HVS testing. Transverse rut profiles were generated to compare the magnitude of shear deformation and densification within each test section. Laboratory-based evaluations were also performed to determine the impact of density on IDT strength and Cantabro loss. Additionally, CTM and DFT measurements were conducted to determine whether a significant difference exists in the MPD and friction number in the test sections before and after HVS testing.

5.1 Impact of In-Place Density on Rutting

Figure 8 shows the progression of rutting within each test section with increasing HVS wheel passes. In general, test section 3 with the highest average in-place density (92.9%) had the lowest average rut depth compared to the other test sections with 86.3% and 90.3% density. The HVS testing was terminated at 100,000 HVS wheel passes.

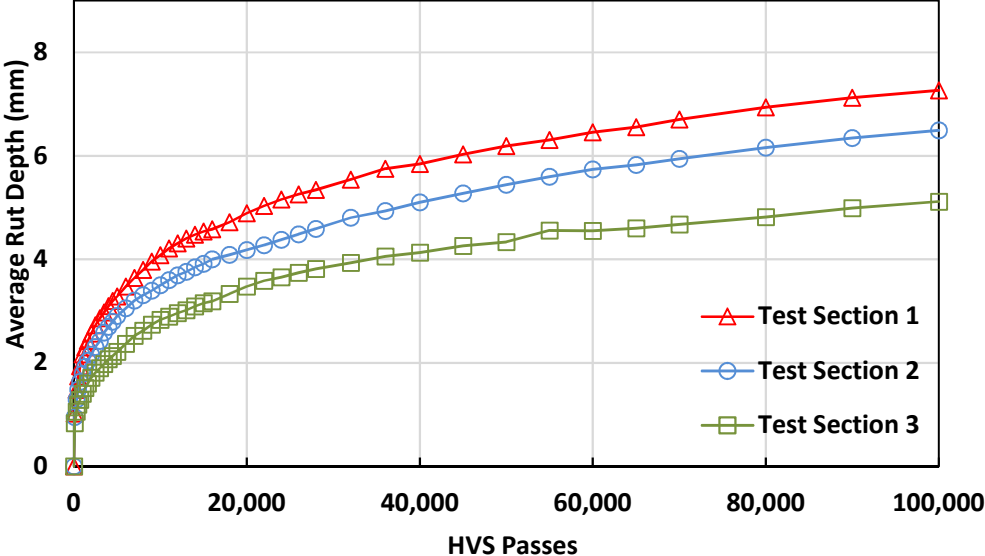


Figure 8. Progression of Rutting Performance in the Test Sections

In previous studies, FDOT researchers determined the portion of rutting generated from shear flow by using the transverse rut profile to estimate the area of accumulated material at the edge of the rutted wheel path and compare it to the channelized area in the wheel path (7, 16). They assumed that the material accumulated at the edge of the rutted wheel path (or hump) is displaced by shear flow. A transverse rut profile with a larger ratio of shear area to wheel path area indicates rutting

is primarily caused by shear and instability rather than densification. The HVS test results show that pavement constructed with higher in-place density experienced less densification and shear deformation.

Figure 9 shows the transverse rut profiles after 100,000 HVS wheel passes for each test section. Table 1 summarizes the rutting performance in terms of densification and shear deformation at increasing HVS wheel pass intervals.

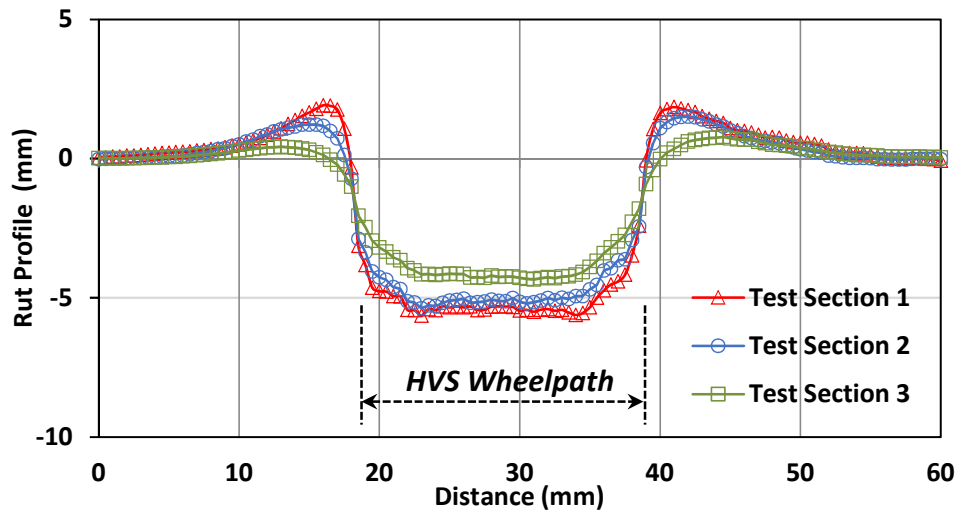


Figure 9. Transverse Rut Profiles at 100,000 HVS Wheel Passes

TABLE 1. Rut Depth Deformation and Densification Summary

Pass Number	Test Section 1		Test Section 2		Test Section 3	
	Avg. Rut, (mm)	Avg. Shear Area /WP Area	Avg. Rut, (mm)	Avg. Shear Area /WP Area	Avg. Rut, (mm)	Avg. Shear Area /WP Area
100	1.02	0.52	0.95	0.25	0.84	0.17
5,000	3.29	0.33	2.91	0.29	2.22	0.20
10,000	4.08	0.39	3.50	0.28	2.83	0.21
20,000	4.89	0.34	4.18	0.27	3.47	0.18
100,000	7.27	0.32	6.49	0.26	5.12	0.15

5.2 Impact of In-Place Density on Cracking Resistance

Figure 10 shows the IDT results for the test sections. Test section 3 with the highest average in-place density had the highest IDT strength results. A simple linear regression represented the correlation between IDT strength and in-place density with an R^2 of 0.90 at the 95% confidence level.

In general, the data show that IDT strength increases with higher in-place density. Although cracking was not observed on any test section during the study, these IDT test results may be indicative of better cracking resistance at higher in-place density.

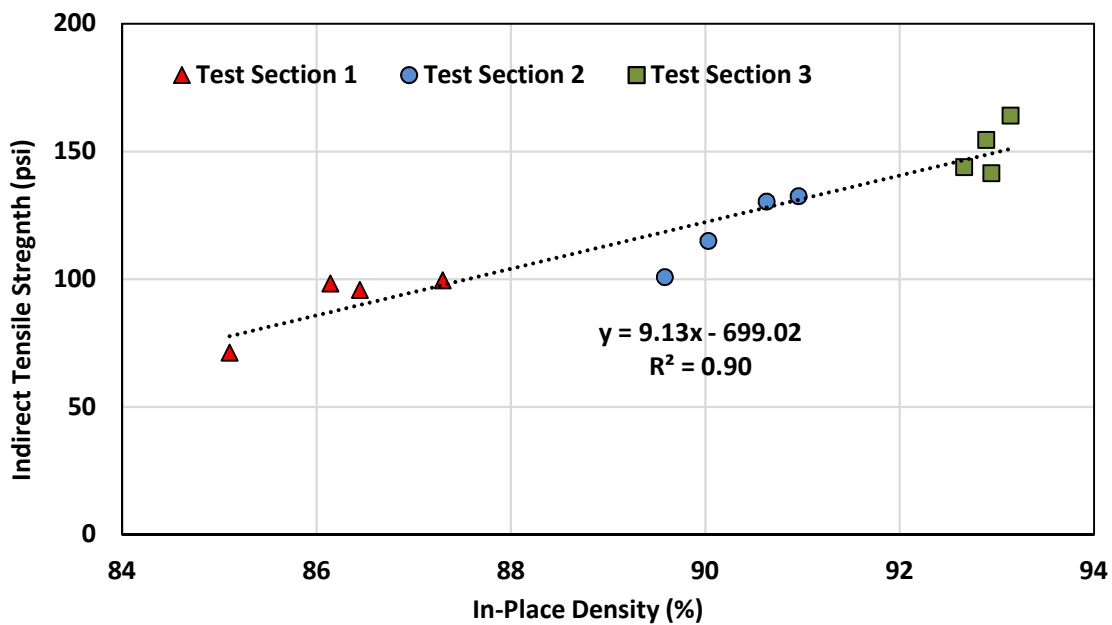


Figure 10. In-Place Density vs Indirect Tensile Strength

5.3 Impact of In-Place Density on Raveling Resistance

Figure 11 shows the Cantabro loss results for the test sections after HVS testing. In general, after HVS testing, test section 3 with the highest average in-place density had the lowest average Cantabro loss at approximately 15.4% compared to 27.8% within test section 1 with the lowest average in-place density. The figure also reflects the increase in average in-place density caused by densification of the loading areas in each test section after HVS testing. A simple linear regression illustrated the correlation between Cantabro loss and in-place density after HVS testing with an R^2 of 0.76 at the 95% confidence level.

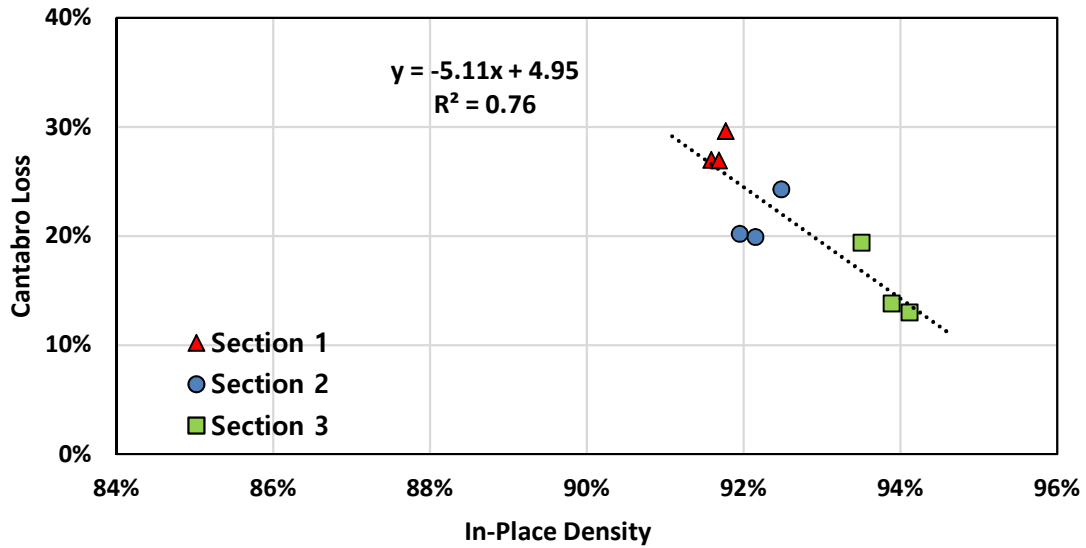


Figure 11. In-Place Density vs. Cantabro Loss After HVS Testing

The average in-place density of the loading areas in test section 1, 2, and 3 increased to 91.7%, 92.2%, and 93.8%, respectively after HVS testing. The results before and after HVS testing are also shown in a tabular form in Table 2. The data show minimal differences in Cantabro loss before and after HVS testing in the test sections.

TABLE 2. Cantabro Abrasion Loss Results

Test Section	Before HVS Testing				After HVS Testing			
	Initial Mass (g)	Mass Loss (g)	Cantabro Loss (%)	Avg. Cantabro Loss (%)	Initial Mass (g)	Mass Loss (g)	Cantabro Loss (%)	Avg. Cantabro Loss (%)
1	571.9	392.8	31.3%	28.2	548.5	400.5	27.0%	27.8
1	565.9	429.8	24.1%		517.5	364.3	29.6%	
1	558.3	395.6	29.1%		509.2	372.1	26.9%	
2	563.0	442.1	21.5%	23.6	537.2	430.2	19.9%	25.5
2	583.1	451.2	22.6%		523.3	417.6	20.2%	
2	576.6	421.8	26.8%		505.9	383.1	24.3%	
3	607.2	520.9	14.2%	13.9	592.8	515.8	13.0%	15.4
3	621.9	533.6	14.2%		566.7	456.9	19.4%	
3	616.4	534.4	13.3%		611.0	526.6	13.8%	

5.4 Impact of In-Place Density on Pavement Surface Macrotexture and Friction

The impact of in-place density on pavement surface macrotexture and friction before and after HVS testing is shown in Figure 12. Overall, the MPD increases in all test sections with increasing HVS wheel passes. However, test section with the highest in-place density had the lowest initial MPD and the least change in MPD after HVS testing. Generally, the friction performance decreased in all test sections with increasing number of HVS wheel passes. However, higher in-place density did not result in better friction performance.

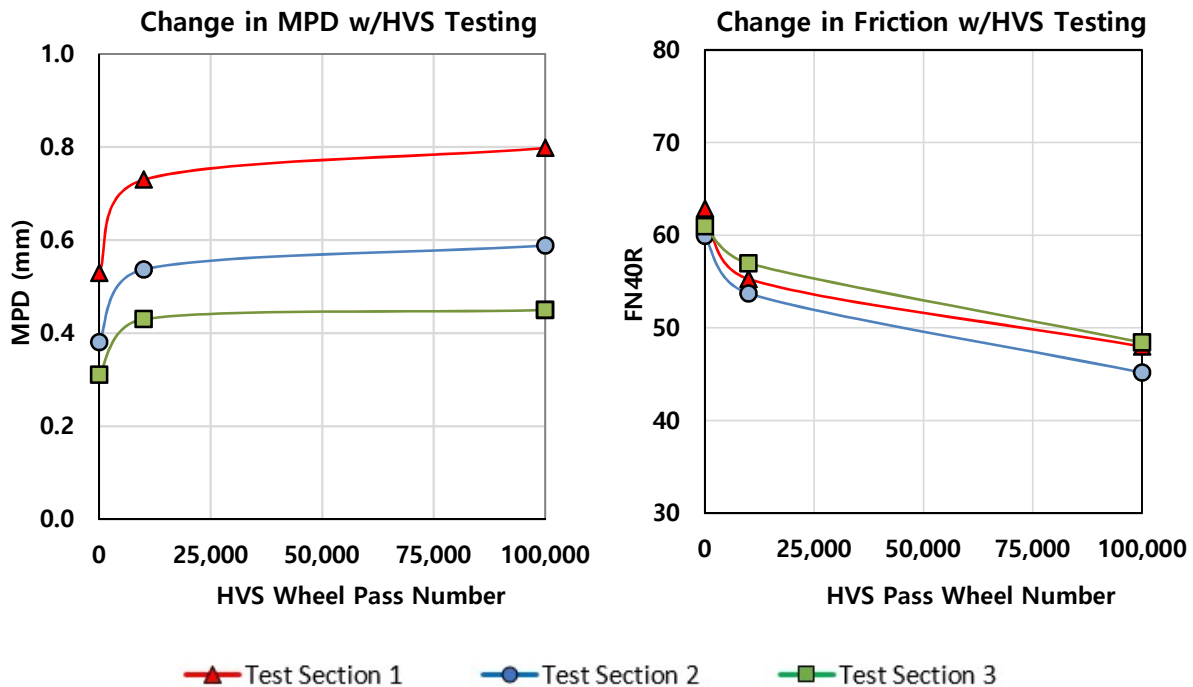


Figure 12. Pavement Surface Macrotexture and Friction Before and After HVS Testing

The greatest change in MPD within all test sections occurred during the first 10,000 HVS wheel passes which may be related to re-orientation of the aggregate structure, since it coincides with the highest rate of rut depth progression during HVS testing previously shown in Figure 8.

The relationship between in-place density and surface texture before and after HVS testing is shown in Figure 13. The pavement density is well correlated with surface texture before and after HVS testing with R^2 values of 0.82 and 0.72, respectively. Previous studies have shown that MPD has a large influence on noise generated from tire-pavement interaction (14). The results from the study show that higher in-place density is well correlated with lower MPD values which is

indicative of lesser noise generated by tire/pavement interaction during the service life of the pavement.

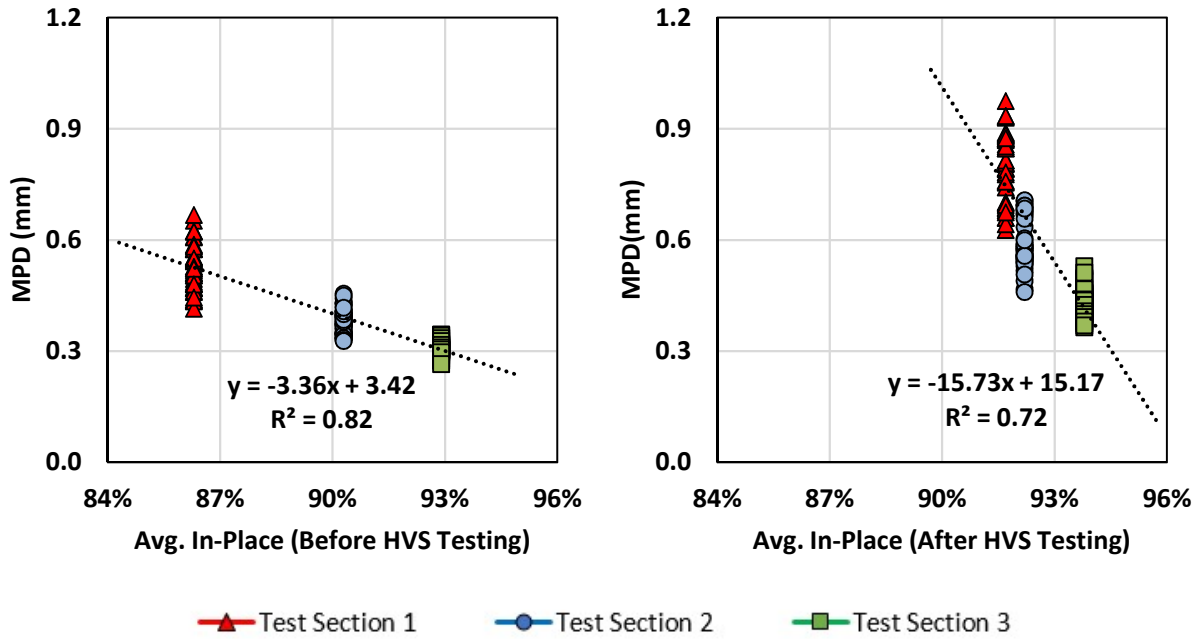


Figure 13. Correlation between In-Place Density and MPD

The descriptive statistics for the MPD measurements in each test section before and after HVS testing are shown in Table 3. The data show that higher in-place density resulted in the least change in pavement surface macrotexture after approximately 100,000 ESALs of traffic loading with the HVS.

TABLE 3. Descriptive Statistics for MPD Data

Test Section	Avg. MPD Before HVS Testing			Avg. MPD After HVS Testing			Avg. MPD Increase after 100,000 HVS passes (mm)
	Avg. (mm)	Std. Dev (mm)	N	Avg. (mm)	Std. Dev (mm)	N	
1	0.54	0.041	45	0.80	0.091	42	0.26
2	0.38	0.034	45	0.59	0.068	38	0.21
3	0.31	0.018	44	0.43	0.039	41	0.12

TABLE 4. Robust Test of Equality of Mean MPD

Condition	Test	F-statistic	df1	df2	Sig.
Before HVS Testing	Welch Test	626.5	2	78	0.000
After HVS Testing	Welch Test	314.1	2	69	0.000

As shown in Table 4, a statistically significant difference in the mean MPD exists among test sections before and after HVS testing as indicated by the result of the Welch tests ($p < 0.001$). The Welch's test is a more robust modification of ANOVA used to determine whether group means are equal even when the data sets being compared have unequal variances and sample sizes (17).

Furthermore, Figure 14 shows that the MPD data collected within each test section shortly after construction are normally distributed. The skewness and kurtosis of the sample data were determined using Jarque-Bera test to measure departure from normality (18).

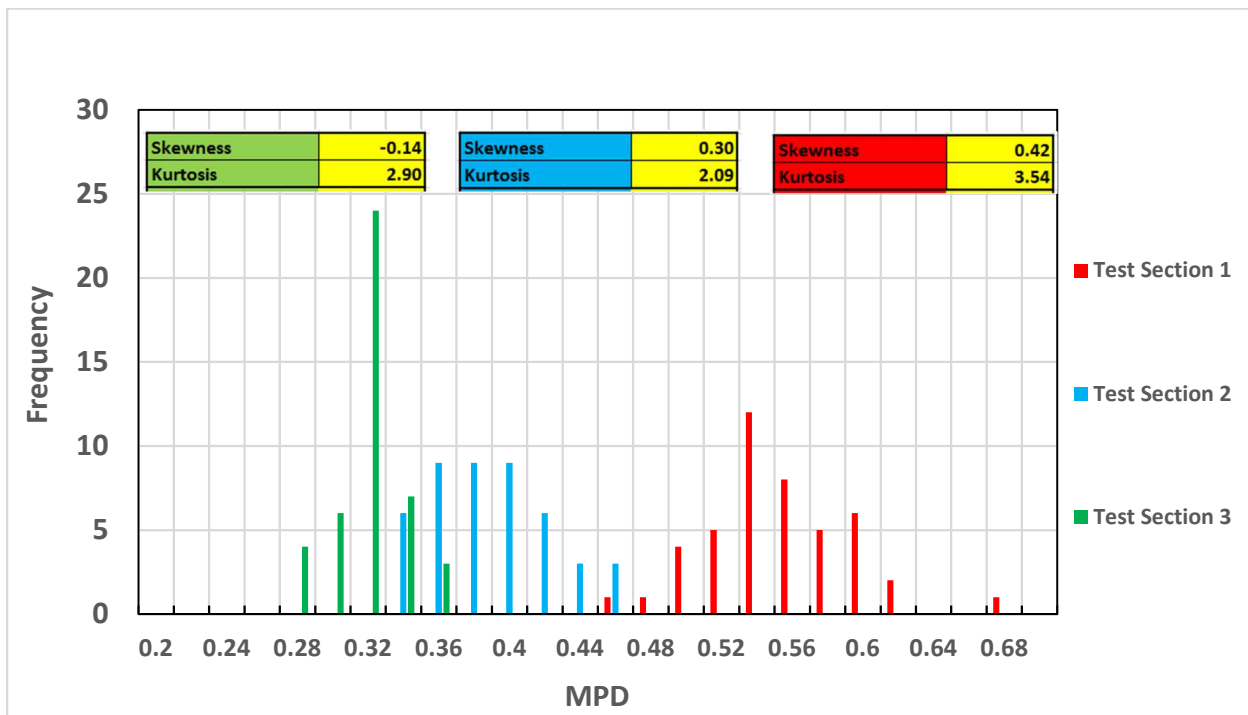


Figure 14. Distribution of MPD on the Test Sections Before HVS Testing

A one-way ANOVA (analysis of variance) F-test is used to conclude whether different group means are equal. A significant F-statistic in an ANOVA only indicates that not all sample means are equal, however it does not indicate which comparison of means are different (19). The Games-Howell procedure was developed to resolve this situation by computing the pair-wise multiple comparison of group means for cases when variances are unequal (20). Tables 5 and 6 below show the pair-wise multiple comparison of mean MPD values before and after HVS testing among the test sections at the 95% confidence level. The data in Table 6 also reflects the increase in the average in-place density of the loading areas in each test section after HVS testing.

TABLE 5. Pair-Wise Multiple Comparison of MPD Before HVS Testing

Test Section (Avg. Density)	Test Section (Avg. Density)	Difference in Mean MPD	Std. Error	Sig.	95% Confidence Level	
					Lower Bound	Upper Bound
1 (86.3%)	2 (90.3%)	0.16	0.008	0.000	0.14	0.18
	3 (92.9%)	0.23	0.007	0.000	0.22	0.25
2 (90.3%)	1 (86.3%)	-0.16	0.008	0.000	-0.18	-0.14
	3 (92.9%)	0.07	0.006	0.000	0.06	0.08
3 (92.9%)	1 (86.3%)	-0.23	0.007	0.000	-0.25	-0.22
	2 (90.3%)	-0.07	0.006	0.000	-0.08	-0.06

TABLE 6. Pair-Wise Multiple Comparison of MPD After HVS Testing

Test Section (Avg. Density)	Test Section (Avg. Density)	Difference in Mean MPD	Std. Error	Sig.	95% Confidence Level	
					Lower Bound	Upper Bound
1 (91.7%)	2 (92.2%)	0.21	0.018	0.000	0.17	0.25
	3 (93.8%)	0.37	0.015	0.000	0.33	0.40
2 (92.2%)	1 (91.7%)	-0.21	0.018	0.000	-0.25	-0.17
	3 (93.8%)	0.16	0.013	0.000	0.13	0.19
3 (93.8%)	1 (91.7%)	-0.37	0.015	0.000	-0.40	-0.33
	2 (92.2%)	-0.16	0.013	0.000	-0.19	-0.13

6 SUMMARY AND CONCLUSIONS

This report described an experimental study carried out to assess the impact of in-place density on the performance of a typical 12.5-mm fine-graded asphalt mixture. The key findings are summarized as follow:

- The HVS testing results indicate that higher in-place density improved asphalt pavement rutting performance. Specifically, the test sections compacted to higher in-place density experienced less densification and shear deformation. The test section compacted to 92.9% density resulted in 21.1% and 29.6% lower rutting depths than the test sections compacted to 90.3% and 86.3% density, respectively.
- Higher pavement density resulted in higher IDT strength, which may be indicative of better cracking resistance. The test section compacted to 92.9% density resulted in 40.8% and 82.9% higher tensile strength than the test sections compacted to 90.3% and 86.3% density, respectively.
- MPD values increased with increasing HVS wheel passes; however, pavement with higher in-place density experienced a lower increase in MPD values after HVS testing.
- Overall, the Cantabro loss decreased with increasing in-place density which may indicate better raveling resistance.

ACKNOWLEDGEMENTS

The work represented herein was the result of a team effort. The authors would like to acknowledge State Materials Office staff from the Pavement Materials and Bituminous Materials Sections for their assistance with data collection, materials testing, and technical advice.

REFERENCES

1. Choubane, B., P. Upshaw, G. Sholar, G. Page, and J. Musselman. Nuclear Density Readings and Core Densities: A Comparative Study. *Transportation Research Record: Journal of the Transportation Research Board*, 1999.1654: 70-78
2. Brown, E. R., and Cross, S. A. *A study of In-Place Rutting of Asphalt Pavements*. National Center for Asphalt Technology. Report 89-02, Auburn, AL, 1989.
3. Harrigan, E.T. Significance of As-Constructed HMA Air Voids to Pavement Performance from Analysis of LTPP Data. *NCHRP Research Results Digest*, 2002. 269: 1-21
4. Zeinali, A., Blankenship, P., and Mahboub, K., Evaluation of the Effect of Density on Asphalt Pavement Durability through Performance Testing., TRB 93rd Annual Meeting Compendium of Papers, 2014.
5. Sebesta, S., Zeig, M., Scullion, T., *Evaluation of Non-Nuclear Density Gauges for HMAC: Year 1 Report.*, Texas Transportation Institute Report 0-4577-1, College Station, TX, 2003
6. Wang, H., Wang, Z., Bennert, T., and Weed, R. *HMA Pay Adjustment*. Report FHWA NJ-2015-007. New Jersey Department of Transportation, 2015.
7. Byron, T., S. Gokhale, and B. Choubane. *Laser Based Technology for Automated Rut Measurement in Accelerated Pavement Testing*. Florida Department of Transportation, 2004.
8. Byron, T., Choubane, B., and Tia, M. Assessing Appropriate Loading Configuration in Accelerated Pavement Testing. Proceedings, 2nd International Conference on Accelerated Pavement Testing, Minneapolis, MN, 2004.
9. Florida Method of Test for Bulk Specific Gravity of Compacted Asphalt Specimens. Florida Sampling and Testing Methods, FM 1-T166. Florida Department of Transportation, 2016.
10. Khosla, N. P., and Harvey, N. *Evaluation of indirect tensile strength as design criteria for Superpave mixtures*. FHWA/NC/2008-02. North Carolina Department of Transportation, 2009.
11. Pérez-Jiménez, F. E., and Calzada-Pérez, M. A. Analysis and Evaluation of the Performance of Porous Asphalt: The Spanish Experience. *Surface Characteristics of Roadways: International Research and Technologies*, 1990. <http://dx.doi.org/10.1520/STP23386S>

12. Doyle, J. D., Howard, I. L., Characterization of Dense-Graded Asphalt with the Cantabro Test, *Journal of Testing and Evaluation*, Vol. 44, No. 1, 2016, pp. 77–88.
13. Flints, G., Leon, E., McGhee, K., and Al-Qadi, I. Pavement Surface Macrotecture Measurement and Applications. *Transportation Research Record: Journal of the Transportation Research Board*, Vol. 1860, pp. 168-177, Washington, D.C., 2014.
14. Rezaei, A., and Harvey, J. T. *Investigation of Noise, Ride Quality and Macrotecture Trends for Asphalt Pavement Surfaces: Summary of Six Years of Measurements*. UCPRC-RR-2013-11. California Department of Transportation, 2013.
15. Choubane, B., Hyung, L., Holzschuher, C., Upshaw, P., Jackson, N., Harmonization of Texture and Friction Measurements on Florida's Open-Graded and Dense-Graded Pavements. *Transportation Research Record: Journal of the Transportation Research Board*, 1999. 2306: 122-130.
16. Greene, J., Toros, U., Kim, S., Byron, T., and Choubane, B., Impact of Wide-Base Tires on Pavement Damage. *Transportation Research Record: Journal of the Transportation Research Board*, Vol. 2155, pp. 82-90. Washington, D.C., 2010.
17. Roth, A. J., Robust Trend Tests Derived and Simulated: Analogs of the Welch and Brown-Forsythe Tests, *Journal of the American Statistical Association*, Vol. 78, No. 384, pp. 972-980, Alexandria, VA, 1983.
18. Mantalos, P., Robust Critical Values for Jarque-Bera Test for Normality, Jonkoping International Business School, Jonkoping University, JIBS Working Papers No. 2010-8., Jonkoping, Sweden, 2010.
19. McClave, J.T., Sincich, T., *Statistics*. Upper Saddle River, NJ: Pearson Prentice Hall, 2006. pp. 512-554.
20. Tamhane, A., A Comparison of Procedures for Multiple Comparisons of Means with Unequal Variances, *Journal of the American Statistical Association*, Vol. 74, No. 366, pp. 471-480, 1979.

APPENDIX

TABLE 7. Indirect Tensile Strength Results

Test Section	Core ID	Density (%)	Tensile strength (psi)	Avg. Density (%)	Avg. Tensile strength (psi)	Tensile Strength Std. Dev. (psi)
1	1	86.4	95.8	86.2	91.2	13.4
	2	85.1	71.3			
	3	86.1	98.4			
	4	87.6	99.6			
2	5	89.6	100.9	90.3	119.7	14.8
	6	91.0	132.5			
	7	90.0	115.0			
	8	90.6	130.4			
3	9	92.7	143.9	92.9	151.0	10.4
	10	92.9	141.5			
	11	93.1	164.1			
	12	92.9	154.6			

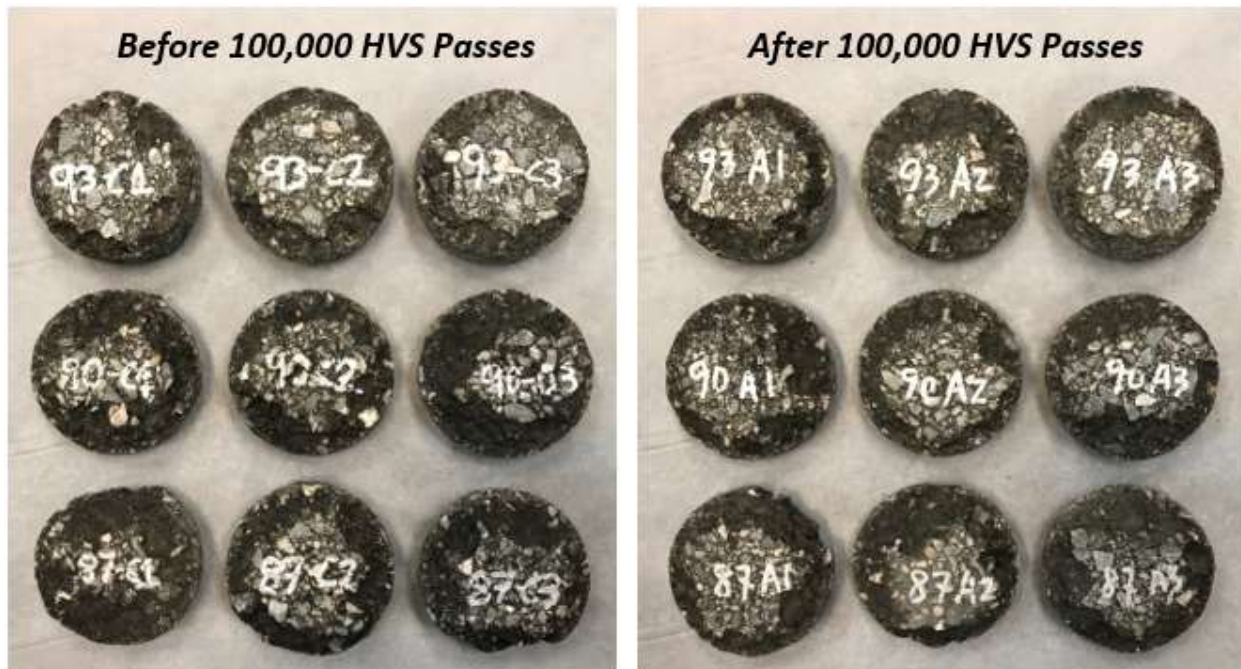


Figure 15. Core Specimens after Cantabro Testing

TABLE 8. Friction Data from DFT Testing

TEST SECTION DENSITY	HVS PASSESS	60 km/h	AVG. FN40R	AVG. DFT60	STD.DEV
87%	0	0.65	62.8	0.66	0.01
	0	0.66			
	0	0.67			
	10,000	0.57	55.4	0.58	0.01
	10,000	0.58			
	10,000	0.58			
	100,000	0.48	48.1	0.49	0.02
	100,000	0.49			
	100,000	0.51			
90%	0	0.63	60.2	0.63	0.00
	0	0.63			
	0	0.63			
	10,000	0.57	53.9	0.56	0.01
	10,000	0.55			
	10,000	0.55			
	100,000	0.48	45.3	0.46	0.03
	100,000	0.48			
	100,000	0.43			
93%	0	0.64	61.1	0.64	0.00
	0	0.65			
	0	0.64			
	10,000	0.59	57.7	0.60	0.02
	10,000	0.62			
	10,000	0.59			
	100,000	0.50	48.8	0.50	0.01
	100,000	0.50			
	100,000	0.51			

**TABLE 9. Aggregate Gradation of Plant Mix Sampled at Test Section 1
(87% Avg. In-Place Density)**

Basket Weight	#	C	Oven No.: NH 580655	3023.4	(A)																																																																																				
Initial Basket + Sample Weight				4554.8	(B)																																																																																				
Initial Sample Weight	(C = B - A)			1531.4	(C)																																																																																				
Extracted Basket + Sample Weight				4474.5	(D)																																																																																				
Extracted Sample Weight (In Basket)	(E = D - A)			1451.1	(E)																																																																																				
Sample Weight Before Washing (After Cleaning Basket)				1451.0	(F)																																																																																				
Washed Sample Weight				1409.6	(G)																																																																																				
Calculated Asphalt Content	(H = ((C - E) / C * 100))			5.24%	(H)																																																																																				
Asphalt Content from Printout				5.28%	(I)																																																																																				
Calibration Factor				-0.19%	(J)																																																																																				
Corrected Asphalt Content	(K = (I + J))			5.09%	(K)																																																																																				
<table border="1"> <thead> <tr> <th>Pass</th> <th>Ret.</th> <th>GRADATION Weight</th> <th>Percent</th> <th>JMF</th> <th></th> </tr> </thead> <tbody> <tr> <td>1 1/2"</td> <td>1"</td> <td></td> <td>0.00</td> <td></td> <td>100.00</td> </tr> <tr> <td>1"</td> <td>3/4"</td> <td></td> <td>0.00</td> <td></td> <td>100.00</td> </tr> <tr> <td>3/4"</td> <td>1/2"</td> <td>22.6</td> <td>1.56</td> <td>100</td> <td>100.00</td> </tr> <tr> <td>1/2"</td> <td>3/8"</td> <td>122.9</td> <td>8.47</td> <td>100</td> <td>98.44</td> </tr> <tr> <td>3/8"</td> <td>#4</td> <td>336.2</td> <td>23.17</td> <td>88</td> <td>89.97</td> </tr> <tr> <td>#4</td> <td>#8</td> <td>327.6</td> <td>22.58</td> <td>64</td> <td>66.80</td> </tr> <tr> <td>#8</td> <td>#16</td> <td>199.9</td> <td>13.78</td> <td>43</td> <td>44.22</td> </tr> <tr> <td>#16</td> <td>#30</td> <td>114.1</td> <td>7.86</td> <td>31</td> <td>30.44</td> </tr> <tr> <td>#30</td> <td>#50</td> <td>118.5</td> <td>8.17</td> <td>21</td> <td>22.58</td> </tr> <tr> <td>#50</td> <td>#100</td> <td>100.8</td> <td>6.95</td> <td>14</td> <td>14.41</td> </tr> <tr> <td>#100</td> <td>#200</td> <td>50.2</td> <td>3.46</td> <td>6</td> <td>7.46</td> </tr> <tr> <td>#200</td> <td>-200</td> <td>16.8</td> <td>4.01</td> <td>4.20</td> <td>4.01</td> </tr> <tr> <td colspan="2">Total -200 (F - G + (-200))</td> <td>41.4</td> <td>+ 16.8</td> <td>=</td> <td>58.2</td> </tr> </tbody> </table>						Pass	Ret.	GRADATION Weight	Percent	JMF		1 1/2"	1"		0.00		100.00	1"	3/4"		0.00		100.00	3/4"	1/2"	22.6	1.56	100	100.00	1/2"	3/8"	122.9	8.47	100	98.44	3/8"	#4	336.2	23.17	88	89.97	#4	#8	327.6	22.58	64	66.80	#8	#16	199.9	13.78	43	44.22	#16	#30	114.1	7.86	31	30.44	#30	#50	118.5	8.17	21	22.58	#50	#100	100.8	6.95	14	14.41	#100	#200	50.2	3.46	6	7.46	#200	-200	16.8	4.01	4.20	4.01	Total -200 (F - G + (-200))		41.4	+ 16.8	=	58.2
Pass	Ret.	GRADATION Weight	Percent	JMF																																																																																					
1 1/2"	1"		0.00		100.00																																																																																				
1"	3/4"		0.00		100.00																																																																																				
3/4"	1/2"	22.6	1.56	100	100.00																																																																																				
1/2"	3/8"	122.9	8.47	100	98.44																																																																																				
3/8"	#4	336.2	23.17	88	89.97																																																																																				
#4	#8	327.6	22.58	64	66.80																																																																																				
#8	#16	199.9	13.78	43	44.22																																																																																				
#16	#30	114.1	7.86	31	30.44																																																																																				
#30	#50	118.5	8.17	21	22.58																																																																																				
#50	#100	100.8	6.95	14	14.41																																																																																				
#100	#200	50.2	3.46	6	7.46																																																																																				
#200	-200	16.8	4.01	4.20	4.01																																																																																				
Total -200 (F - G + (-200))		41.4	+ 16.8	=	58.2																																																																																				

**TABLE 10. Aggregate Gradation of Plant Mix Sampled at Test Section 2
(90% Avg. In-Place Density)**

Basket Weight	#	A	Oven No.: NH 580655	3077.1	(A)
Initial Basket + Sample Weight				4778.6	(B)
Initial Sample Weight		(C = B - A)		1701.5	(C)
Extracted Basket + Sample Weight				4692.2	(D)
Extracted Sample Weight (In Basket)		(E = D - A)		1615.1	(E)
Sample Weight Before Washing (After Cleaning Basket)				1615.1	(F)
Washed Sample Weight				1562.4	(G)
Calculated Asphalt Content		(H = ((C - E) / C * 100))		5.08%	(H)
Asphalt Content from Printout				5.22%	(I)
Calibration Factor				-0.19%	(J)
Corrected Asphalt Content		(K = (I + J))		5.03%	(K)
GRADATION					
Pass	Ret.	Weight	Percent	JMF	
1 1/2"	1"		0.00		100.00
1"	3/4"		0.00		100.00
3/4"	1/2"	3.3	0.20	100	100.00
1/2"	3/8"	111.5	6.90	100	99.80
3/8"	#4	410.4	25.41	88	92.90
#4	#8	366.2	22.67	64	67.49
#8	#16	224.8	13.92	43	44.82
#16	#30	130.0	8.05	31	30.90
#30	#50	134.2	8.31	21	22.85
#50	#100	113.3	7.02	14	14.54
#100	#200	56.1	3.47	6	7.52
#200	-200	12.3	4.02	4.20	4.02
Total -200 (F - G + (-200))		52.7	+ 12.3	=	65.0

**TABLE 11. Aggregate Gradation of Plant Mix Sampled at Test Section 3
(93% Avg. In-Place Density)**

Basket Weight	#	D	Oven No.: NH 581201	3098.6	(A)																																																																																				
Initial Basket + Sample Weight				4751.3	(B)																																																																																				
Initial Sample Weight	(C = B - A)			1652.7	(C)																																																																																				
Extracted Basket + Sample Weight				4664.8	(D)																																																																																				
Extracted Sample Weight (In Basket)	(E = D - A)			1566.2	(E)																																																																																				
Sample Weight Before Washing (After Cleaning Basket)				1566.0	(F)																																																																																				
Washed Sample Weight				1513.6	(G)																																																																																				
Calculated Asphalt Content	(H = ((C - E) / C * 100))			5.23%	(H)																																																																																				
Asphalt Content from Printout				5.20%	(I)																																																																																				
Calibration Factor				-0.19%	(J)																																																																																				
Corrected Asphalt Content	(K = (I + J))			5.01%	(K)																																																																																				
<table border="1"> <thead> <tr> <th>Pass</th> <th>Ret.</th> <th>GRADATION Weight</th> <th>Percent</th> <th>JMF</th> <th></th> </tr> </thead> <tbody> <tr> <td>1 1/2"</td> <td>1"</td> <td></td> <td>0.00</td> <td></td> <td>100.00</td> </tr> <tr> <td>1"</td> <td>3/4"</td> <td></td> <td>0.00</td> <td></td> <td>100.00</td> </tr> <tr> <td>3/4"</td> <td>1/2"</td> <td>23.5</td> <td>1.50</td> <td>100</td> <td>100.00</td> </tr> <tr> <td>1/2"</td> <td>3/8"</td> <td>134.4</td> <td>8.58</td> <td>100</td> <td>98.50</td> </tr> <tr> <td>3/8"</td> <td>#4</td> <td>358.4</td> <td>22.89</td> <td>88</td> <td>89.92</td> </tr> <tr> <td>#4</td> <td>#8</td> <td>352.9</td> <td>22.54</td> <td>64</td> <td>67.03</td> </tr> <tr> <td>#8</td> <td>#16</td> <td>216.4</td> <td>13.82</td> <td>43</td> <td>44.49</td> </tr> <tr> <td>#16</td> <td>#30</td> <td>125.8</td> <td>8.03</td> <td>31</td> <td>30.67</td> </tr> <tr> <td>#30</td> <td>#50</td> <td>128.2</td> <td>8.19</td> <td>21</td> <td>22.64</td> </tr> <tr> <td>#50</td> <td>#100</td> <td>108.3</td> <td>6.92</td> <td>14</td> <td>14.45</td> </tr> <tr> <td>#100</td> <td>#200</td> <td>53.9</td> <td>3.44</td> <td>6</td> <td>7.53</td> </tr> <tr> <td>#200</td> <td>-200</td> <td>11.2</td> <td>4.06</td> <td>4.20</td> <td>4.06</td> </tr> <tr> <td colspan="2">Total -200 (F - G + (-200))</td> <td>52.4</td> <td>+ 11.2</td> <td>=</td> <td>63.6</td> </tr> </tbody> </table>						Pass	Ret.	GRADATION Weight	Percent	JMF		1 1/2"	1"		0.00		100.00	1"	3/4"		0.00		100.00	3/4"	1/2"	23.5	1.50	100	100.00	1/2"	3/8"	134.4	8.58	100	98.50	3/8"	#4	358.4	22.89	88	89.92	#4	#8	352.9	22.54	64	67.03	#8	#16	216.4	13.82	43	44.49	#16	#30	125.8	8.03	31	30.67	#30	#50	128.2	8.19	21	22.64	#50	#100	108.3	6.92	14	14.45	#100	#200	53.9	3.44	6	7.53	#200	-200	11.2	4.06	4.20	4.06	Total -200 (F - G + (-200))		52.4	+ 11.2	=	63.6
Pass	Ret.	GRADATION Weight	Percent	JMF																																																																																					
1 1/2"	1"		0.00		100.00																																																																																				
1"	3/4"		0.00		100.00																																																																																				
3/4"	1/2"	23.5	1.50	100	100.00																																																																																				
1/2"	3/8"	134.4	8.58	100	98.50																																																																																				
3/8"	#4	358.4	22.89	88	89.92																																																																																				
#4	#8	352.9	22.54	64	67.03																																																																																				
#8	#16	216.4	13.82	43	44.49																																																																																				
#16	#30	125.8	8.03	31	30.67																																																																																				
#30	#50	128.2	8.19	21	22.64																																																																																				
#50	#100	108.3	6.92	14	14.45																																																																																				
#100	#200	53.9	3.44	6	7.53																																																																																				
#200	-200	11.2	4.06	4.20	4.06																																																																																				
Total -200 (F - G + (-200))		52.4	+ 11.2	=	63.6																																																																																				

TABLE 12. Asphalt Binder Laboratory Test Results

Bituminous Laboratory	Report of Grading Results for PG 76 Binders	Effective Date: July 1, 2013	
		By: MS	Page 1 of 1

STATE OF FLORIDA DEPARTMENT OF TRANSPORTATION
BITUMINOUS MATERIAL REPORT

Project: HVS-9 Test Track

Sample Type: 76-22(PMA)

Lab No.: 16020-LB

Test	Test Temperature	Test Results	SPECIFICATION	
<i>Tests on Original Binder</i>				
Separation Test (ARB only)	N/A	N/A	Max. Difference, 15°F	
Solubility, % (PMA only)	N/A	99.50	Min. 99.0%	
Flash Point, COC	N/A	500+	Min. 450°F	
Rotational Viscosity	135°C	1.53	Max. 3 Pa·s	
DSR, G*/sin δ, @ 10 rad/s	76°C	1.53	Min. 1.0 kPa	
Phase Angle		69.6	Max. 75 degrees	
DSR, G*/sin δ, @ 10 rad/s	82°C	0.79	Min. 1.0 kPa	
Phase Angle		72.0	Max. 75 degrees	
<i>Tests on Residue from Rolling Thin Film Oven Test</i>				
RTFOT, Mass Change	163°C	-0.474	Max. ± 1.00%	
MSCR	67°C	R _{3.2}	66.41	
		J _{nr3.2}	0.302	Max. 1.00 kPa
		J _{nr diff}	37.56	Max. 75%
		% Recovery	Pass	%R _{3.2} > 40.25
High Temperature Grade:				
<i>Pressure Aging Vessel Tests</i>	100°C	<i>Tests on Residue from PAV</i>		
DSR, G* sin δ, @ 10 rad/s	26.50°C	2470	Max. 5000 kPa	
BBR, Creep Stiffness, S	-12°C	131	Max. 300 MPa	
Creep Stiffness, M-value		0.329	Min. 0.300	
Note:	This sample passed Florida Department of Transportation high temperature specification for Performance Graded Binder, PG 76-22(PMA). True Grade: 79.3			